Computers in Biology and Medicine 134 (2021) 104515

Contents lists available at ScienceDirect

Computers in Biology and Medicine

journal homepage: www.elsevier.com/locate/compbiomed

Effective connectivity in brain networks estimated using EEG signals is altered in children with ADHD

Ali Kareem Abbas [a], Ghasem Azemi [a,b,*], Sajad Amiri [a], Samin Ravanshadi [a], Amir Omidvarnia [c,d]

[a] Faculty of Electrical and Computer Engineering, Razi University, Kermanshah, Iran
[b] Department of Cognitive Science, Faculty of Medicine, Health and Human Sciences, Macquarie University, Sydney, Australia
[c] Institute of Bioengineering, Center for Neuroprosthetics, Center for Biomedical Imaging, EPFL, Lausanne, Switzerland
[d] Department of Radiology and Medical Informatics, University of Geneva, Geneva, Switzerland

ARTICLE INFO

Keywords:
EEG
Brain connectivity analysis
ADHD
Transfer entropy
Network measures

ABSTRACT

This study presents a methodology developed for estimating effective connectivity in brain networks (BNs) using multichannel scalp EEG recordings. The methodology uses transfer entropy as an information transfer measure to detect pair-wise directed information transfer between EEG signals within δ, θ, α, β and γ-bands. The developed methodology is then used to study the properties of directed BNs in children with attention-deficit hyperactivity disorder (ADHD) and compare them with that of the healthy controls using both statistical and receiver operating characteristic (ROC) analyses. The results indicate that directed information transfer between scalp EEG electrodes in the ADHD subjects differs significantly compared to the healthy ones. The results of the statistical and ROC analyses of frequency-specific graph measures demonstrate their highly discriminative ability between the two groups. Specifically, the graph measures extracted from the estimated directed BNs in the β-band show the highest discrimination between the ADHD and control groups. These findings are in line with the fact that β-band reflects active concentration, motor activity, and anxious mental states. The reported results show that the developed methodology has the capacity to be used for investigating patterns of directed BNs in neuropsychiatric disorders.

1. Introduction

Analysis of functional integration in the brain is a multidisciplinary field of research which looks into the dynamical interactions between brain regions. These relationships can be divided into two general classes of functional and effective connections [1]. Functional connectivity studies the statistical dependencies between the dynamics of brain areas. Effective connectivity, on the other hand, indicates the causal interactions between activated brain regions and describes the directional effects one neuronal system in the brain exerts upon another. Integrative and multimodal analyses of brain connectivity can potentially lead to enhanced neurologic principles by validating and extending pathophysiological concepts. Effective connectivity in the context of brain dynamics refers to causal functional interactions between regions of the brain; that is, to the direct effect on another region of one region of the brain. To determine effective connectivity, the variation of neuronal activity within one area of the brain and measurements of responses in remote areas can be used. These variations can be achieved under certain assumptions regarding their effects by delivering carefully controlled stimuli or by procedures such as neuroimaging. Obviously, the type of connectivity to be analyzed and the use of integrative methods depend on the purpose of the study, brain function and research assumptions [1–3].

Attention-deficit hyperactivity disorder (ADHD) is a highly prevalent disorder of childhood characterized by inattention, hyperactivity and impulsivity [4]. Children with ADHD suffer from weak behavioral management and control, so that they often show relevant reactions to various stimuli [5–8]. ADHD is diagnosed by a set of criteria outlined in the Diagnostic and Statistical Manual of Mental Disorders IV Text Revision (DSM-IV-TR), and International Classification of Diseases (ICD-10) [9,10]. Those diagnostic criteria are measured through cognitive functional tests and behavioral observations.

Cortical activity in one part of the brain and its causal relationship with responses in other brain areas can be quantified through effective connectivity analysis of functional magnetic resonance imaging (fMRI), magnetoencephalography (MEG), and electroencephalography (EEG)

* Corresponding author. Department of Cognitive Science, Faculty of Medicine, Health and Human Sciences, Macquarie University, Sydney, Australia.
E-mail address: g.azemi@razi.ac.ir (G. Azemi).

https://doi.org/10.1016/j.compbiomed.2021.104515
Received 14 February 2021; Received in revised form 16 May 2021; Accepted 21 May 2021
Available online 1 June 2021

[11–13].

Effective connectivity studies have revealed neural mechanisms and pathways in humans' brain networks (BNs) during task engagement including attention [14], visual pursuit [15], reading [16], cerebro-cerebellar visual processing of body motion [17], memory retrieval [18] and mental imagery [19]. Such analyses have, therefore, been used to investigate brain function of patients with neuropsychiatric conditions such as ADHD. Abnormal features of effective brain connectivity in ADHD patients have already been postulated from the pathophysiological perspective [20]. For example, Sripada et al. [21] hypothesized the presence of abnormal network interconnections in patients with ADHD. Most of the previous studies have used EEG, MEG, and fMRI data to evaluate functional connectivity in ADHD subjects [22–26]. Alba et al. [22] showed that although there is no statistically significant difference between average functional connectivity of the ADHD cohort and healthy subjects, its variability is statistically greater in the patients group. Khadmaoui et al. [23] argued that the interactions between EEG channels at rest are stronger in ADHD patients compared to the healthy control subjects at frontal regions and in all EEG frequency bands. The functional linkage between regions of interests in fMRI recordings of ADHD and its link with brain structure was studied in [24]. The analysis of functional brain connectivity in ADHD and non-ADHD subjects in [25] addressed brain cognition and brain disorders in ADHD patients. In [26], the structural and functional BNs in the ADHD cases and their pathophysiological substrates were investigated. It is important to note that the majority of previous EEG studies of ADHD have examined functional connectivity within low frequency bands. However, there is an increasing evidence showing the contribution of high frequency EEG activities in memory and attention [27,28]. This observation has led to a number of studies on effective connectivity analysis of ADHD at higher frequency bands of EEG [29–31]. In [32], a significant bidirectional information flow was shown between EEG channels through effective connectivity analysis in the time and frequency domains. The impact of spectral content on functional and causal relationships between scalp EEG channels in ADHD is still an open question. In the most recent related paper, published while this manuscript was being revised, different information pathways of BNs were investigated in children with ADHD in comparison with healthy subjects [33]. This study has used the same database as the one in the current work and has shown that directed information flow between brain regions, it is likely disrupted in children with ADHD, and this change is frequency-specific.

The increasing usage of EEG-derived brain connectivity analysis in ADHD studies over the recent years implies the salient capacity of this approach for better understanding of ADHD and its impact on EEG recordings. In particular, effective connectivity analysis of scalp EEG provides an affordable, non-invasive and temporally high-resolution measurement to study directional and non-directional interactions between cortical regions of ADHD patients. This paper investigates effective connectivity in a group of 56 ADHD patients in contrast to 56 control subjects through measuring of the information flow between scalp EEG channels using transfer entropy (TE) [34]. The aim is to explore the impact of ADHD on the graph features of EEG-based directed BNs. Transfer entropy between EEG channels is used to generate directed brain graphs in the two groups. The differences between the BNs are studied in the five standard EEG frequency bands. In this way, we look into the impact of EEG frequency bands on the effective connectivity of ADHD versus healthy subjects from the perspective of graph theory.

The rest of the paper is organized as follows: Section 2 describes the multichannel EEG database used in this study and introduces the adapted analysis framework for estimating directed BNs using multichannel scalp EEG signals. In Section 3, the experimental results of applying the proposed methodology to the EEG database are presented and discussed in Section 4. The paper is concluded in Section 5.

2. Materials and methods

2.1. The EEG database

This study used a newly released database consisting of scalp-level multichannel EEG signals collected from 121 children [35]. The signals were recorded at the sampling rate of 128 Hz using a 19-channel montage, i.e. Fp1, Fp2, F3, F4, C3, C4, P3, P4, O1, O2, F7, F8, T3, T4, T5, T6, Fz, Cz, and Pz, according to the 10–20 international system of EEG electrode placement. Eye movements were recorded by two electrodes that were placed below and above the right eye. An EEG recording protocol was designed according to the behavior of ADHD children based on the visual attention tasks [36]. The images of cartoon characters were shown to the children and the subjects were asked to count the number of characters during the EEG recording. Each randomly selected image had between five to 16 characters and the image size was big enough for children to see and count. In order to achieve an ongoing stimulus during signal capture, the images were displayed immediately and continuously after the child's response. Therefore, the duration of each EEG recording over the course of this cognitive visual task was dependent on the performance of the child. Note that the database does not provide the number of incorrect answers provided by the subjects or any information about the behavior rating scales for the ADHD subjects.

Amongst the 121 subjects, 61 children were diagnosed as having ADHD by an experienced psychiatrist based on the guidelines in the American Psychiatric Association's Diagnostic and Statistical Manual, 4th edition (DSM-IV) [37]. The remaining 60 children participated as healthy controls voluntarily and were checked to have no particular psychological disorder, epilepsy or head injury. More details about this EEG database can be found in [35]. In this study, we used 56 EEG datasets from each group and fed them into the pre-processing stage.

2.2. Methods

The analysis framework in this study consists of the following steps: (*i*) pre-processing, (*ii*) construction of weighted directed BNs, (*iii*) graph analysis, and (*iv*) statistical and ROC analyses. The block diagram of the adapted framework is depicted in Fig. 1.

2.2.1. Pre-processing

The removal of physiological and non-physiological artifacts such as high-amplitude changes of EEG due to eye movement is a crucial step for extraction of meaningful information from multichannel EEG recordings. In order to enhance the EEG signals, we first applied a zero phase Butterworth filter of order 50 in the 0.5–45 Hz frequency band. We then used a stationary wavelet transform (SWT) to enhance EEG datasets more and extract $\boldsymbol{\delta}$ (0.5–4 Hz), $\boldsymbol{\theta}$ (4–8 Hz), $\boldsymbol{\alpha}$ (8–13 Hz), $\boldsymbol{\beta}$ (13–30 Hz), and $\boldsymbol{\gamma}$ (30–45 Hz) frequency bands. The SWT utilizes recursively dilated filters in order to halve the bandwidth from one level to another, so it is suitable for highlighting the spectral features of EEG in different frequency bands [38]. It is a translation-invariance modification of the Discrete Wavelet Transform that does not decimate coefficients at every transformation level, i.e. the approximation and details coefficients at all levels have the same length as the original signal. In this study, the SWT was implemented using the Haar wavelet as the mother wavelet and the decomposition level was chosen to be 5. Note that this choice of the decomposition level, given the fact that the sampling frequency of the EEG signals is 128 Hz, allows for the extraction of $\boldsymbol{\delta}, \boldsymbol{\theta}, \boldsymbol{\alpha}, \boldsymbol{\beta}$ and $\boldsymbol{\gamma}$ frequency bands. Finally, all EEG channels in each dataset were visually inspected and the intervals with remaining artifacts were removed manually.

The first 1-min segment from the pre-processed multichannel EEG datasets of each group was chosen for analysis. Note that the EEG signals used in this study were recorded while the subjects were performing a continuous cognitive visual task, i.e. under continuous stimulus. This

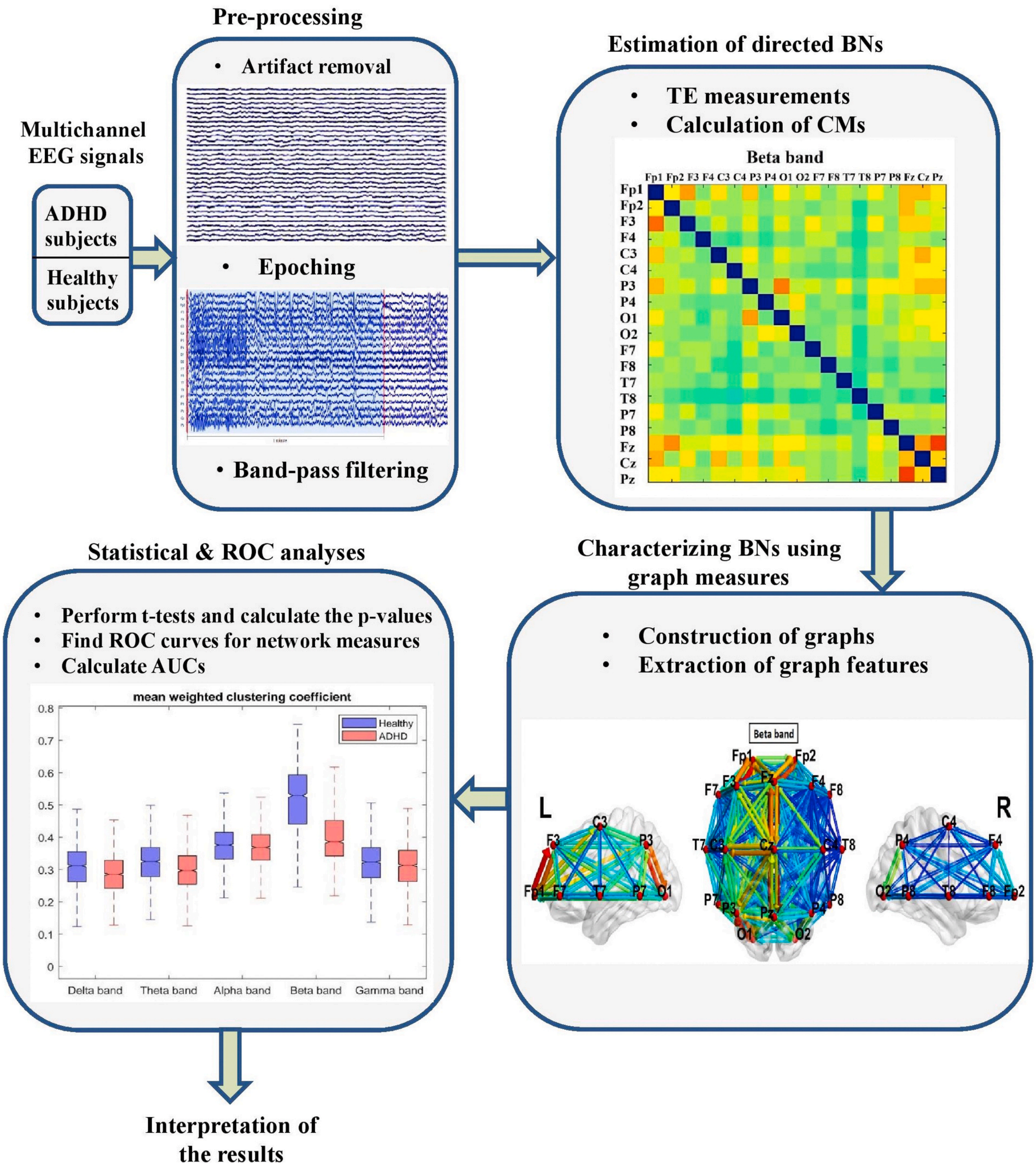

Fig. 1. Block diagram of the methodology used in this study for estimation and analysis of directed BNs in ADHD and healthy control subjects. Abbreviations: TE: transfer entropy, CM: connectivity matrix, ROC: receiver operating characteristic, and AUC: area under the ROC curve.

was achieved by displaying each image immediately and uninterruptedly after the subject's response. The 1-min segment was then divided into 3-s overlapping windows (containing 384 samples) with 1-s overlap between successive windows; resulting in 29 sliding windows for each subject. The duration of EEG segments was chosen based on the previous studies in this field [29,35]. See Table 1 for more information about the selected EEG datasets in this study.

2.2.2. Estimation of directed BNs from multichannel EEG

From each multichannel EEG segment, the directed BNs were estimated using pair-wise TE and analyzed in five commonly used EEG frequency bands, i.e., δ, θ, α, β, and γ frequency bands.

2.2.2.1. Transfer entropy. Pair-wise transfer entropy (TE) was used to quantify the directional relationship between scalp EEG channels [39]. TE estimates linear and nonlinear connections between two signals by measuring the amount of data transferred into each direction between them [39]. It has, therefore, become an inviting choice for the estimation of BNs using multichannel EEG [40]. Let X and Y be two EEG channels which are assumed to be of k^{th} and l^{th} order Markov processes, i.e., each sample of X and Y at time t depends only on its past k and l samples, respectively. In other words, the two random processes are embedded in a reconstructed phase space with the dimension of k and l, respectively. Therefore, X and Y can be represented as a set of k- and l-dimensional reconstructed state vectors denoted as $X_t^{(k)} = (X_t, X_{t-1}, \ldots$

Table 1
Details about the selected EEG datasets used in this study. Subject IDs are in accordance with the indexing of subjects in [35].

Group	Subject IDs of the selected datasets	Dataset length in seconds (min – max)
ADHD	1, 3, 6, 8, 10, 12, 14, 18, 19, 21, 22, 24, 27, 28, 29, 30, 31, 32, 33, 34, 35, 36, 37, 38, 39, 40, 173,177, 179, 181, 183, 190, 196, 198, 200, 204, 206, 209, 213, 215, 219, 227, 234, 236, 238, 244, 246, 250, 254, 263, 265, 270, 274, 279, 284, 288.	(63–283)
Healthy control	41,42, 43, 44, 45, 46, 47, 49, 50, 52, 53, 54, 56, 57, 58, 59, 60, 107, 108, 109, 110, 111, 112, 113, 114, 115, 116, 117, 118, 120, 121, 123, 125, 127, 129, 131, 133, 134, 138, 140, 143, 147, 151, 297, 298, 299, 300, 302, 303, 304, 305, 306, 307, 308, 309, 310.	(70–178)

$, X_{t-k+1})$ and $\boldsymbol{Y}_t^{(l)} = (Y_t, Y_{t-1}, \ldots, Y_{t-l+1})$, respectively. In this case, the transfer of information flow from channel $\boldsymbol{X}$ to channel $\boldsymbol{Y}$ is defined as the ratio of the conditional distribution of $\boldsymbol{Y}$ with respect to the past samples of $\boldsymbol{X}$ and $\boldsymbol{Y}$ versus the conditional distribution of $\boldsymbol{Y}$ depending only on its own past [41]:

$$TE_{X\to Y} = T\left(Y_{t+1} \middle| \boldsymbol{X}_t^{(k)}, \boldsymbol{Y}_t^{(l)}\right) = \sum_{Y_{t+1}, \boldsymbol{Y}_t^{(l)}, \boldsymbol{X}_t^{(k)}} p\left(Y_{t+1}, \boldsymbol{X}_t^{(k)}, \boldsymbol{Y}_t^{(l)}\right) \log\left(\frac{p\left(Y_{t+1} \middle| \boldsymbol{Y}_t^{(l)}, \boldsymbol{X}_t^{(k)}\right)}{p\left(Y_{t+1} \middle| \boldsymbol{Y}_t^{(l)}\right)}\right) \tag{1}$$

where $p(Y_{t+1}, \boldsymbol{X}_t^{(k)}, \boldsymbol{Y}_t^{(l)})$ represents the joint probability density function (PDF) of Y_{t+1}, $\boldsymbol{X}_t^{(k)}$, and $\boldsymbol{Y}_t^{(l)}$ values, and $p(Y_{t+1}|\boldsymbol{Y}_t^{(l)}, \boldsymbol{X}_t^{(k)})$ and $p(Y_{t+1}|\boldsymbol{Y}_t^{(l)})$, respectively, represent conditional PDFs of Y_{t+1} given the past information of $\boldsymbol{Y}_t^{(l)}$ and $\boldsymbol{X}_t^{(k)}$ as well as $\boldsymbol{Y}_t^{(l)}$ only. A value of $TE_{X\to Y} = 0$ indicates that $\boldsymbol{X}$ transfers no information to $\boldsymbol{Y}$. Also, it is clear from the definition of $TE_{X\to Y}$ that $TE_{X\to Y}$ and $TE_{Y\to X}$ are not necessarily equal. For calculating the transfer entropy between any two channels, this study used the value of 1 for both k and l. This choice is supported by other studies, e.g. [41,42], which have found that these values are especially appropriate in biomedical experiments where time series length is usually short and the absolute values of auto-correlation functions tend to decrease monotonically as time lag increases.

In order to normalize the directional relationship between each pair of EEG channels and set the maximum $TE_{X\to Y}$ values to 1, the normalized transfer entropy $NTE_{X\to Y}$ was defined as follows:

$$NTE_{X\to Y} = \frac{TE_{X\to Y}}{(TE_{X\to Y} + TE_{Y\to X})} \in [0, 1]. \tag{2}$$

In this study, we used the definition of $NTE_{X\to Y}$ to develop a frequency-specific time-varying connectivity matrix ($\boldsymbol{CM}$) for sliding-windowed multichannel EEG recordings of each subject. The matrix is defined as follows:

$$\boldsymbol{CM} = [NTE_{X,Y}] \in \mathbb{R}^{19\times 19\times N_w} \tag{3}$$

where N_w is the number of EEG segments in the dataset and CM_{ij}^w is associated with the normalized transfer entropy from the i^{th} EEG channel to the j^{th} EEG channel in the w^{th} sliding window. In fact, $\boldsymbol{CM}$ serves as a time-varying directional brain graph with 19 nodes for each EEG dataset in five EEG frequency bands. The rows of $\boldsymbol{CM}$ at each window indicate the strength of the outgoing connections from the i^{th} node to the j^{th} node and the columns of $\boldsymbol{CM}$ indicate the strength of the incoming connections to the i^{th} node from the j^{th} node. The directed brain graphs $\boldsymbol{CM}$ for all subjects in the ADHD and healthy groups were computed (five graphs per subject associated with five EEG frequency bands) and six undirected graph measures were extracted from them to investigate the network differences between directed BNs of the two groups.

2.2.3. Characterizing BNs using graph measures

In this study, six graph measures were used to quantify network features of causal interactions between EEG channels at the local and global scales covering both integration and segregation aspects of functional information flow in cortical dynamics. A brief description of the graph measures used in this study is followed, while more details can be found in [43–46].

1. Global efficiency (GE) is defined as the average inverse shortest path length between all node pairs in the graph. High global efficiency means that connections can easily exchange information across the entire graph.
2. Mean weighted clustering coefficient (MWCC) is calculated as the ratio of the number of triangles around a node to the number of possible triplets around that node averaged over all nodes in the graph. High MWCC shows a high probability that the neighboring nodes are interrelated and connected.
3. Average degree (AD) is calculated as the average number of connections across the rows of the graph (indicating the out-degree) and the number of connections across the columns of the graph (indicating the in-degree). High average degree means that the graph has more connections and therefore, information can move faster from one node to another.
4. Mean strength (MS) is the average strength of all nodes in the graph, where the strength of a node is defined as the sum of the edge weights associated with that node. MS values depend on the number of in- and out-edge weights for all node-related connections.
5. Transitivity (Tr) reveals the existence of tightly connected clusters in the graph by measuring the overall probability for the graph to have adjacent nodes interconnected. Maximum value of Tr is 1 which means that the graph contains all possible edges.
6. Path length (PL) is calculated as the average distance from a node to all other nodes in the graph. High path length means the graph has long connection between nodes.

2.2.4. Statistical and ROC analyses

Once the directed BNs were constructed and the graph measures were extracted from them, the measures representing directed BNs for the two groups were compared through a rigorous statistical testing. As mentioned in Section 2.2.3, six graph measures were extracted from the constructed directed BN of each 3-s 19-channel EEG segment in five different frequency bands. This resulted in $29 \times 56 = 1624$ values, i.e. the number of 3-s segments for each subject times the number of subjects in each group, for each graph measure in each frequency band for each group. In order to check whether the extracted graph measures for ADHD and healthy control subjects and therefore, the constructed BNs are statistically different, we carried out the t-test on the 1624 values of each feature for the two groups in different frequency bands, i.e. $\boldsymbol{\delta}, \boldsymbol{\theta}, \boldsymbol{\alpha}, \boldsymbol{\beta}$ and $\boldsymbol{\gamma}$. We also used each graph measure in each frequency band to classify the two groups, computed the sensitivity (SEN) and the specificity (SPE) for each measure and calculated the area under the receiver operating characteristic (ROC) curve, i.e. AUC, as a criterion of the capacity of a particular measure for discrimination between the two groups. The entire analysis framework was implemented in MATLAB and the graph measures were extracted using the Brain Connectivity Toolbox [47].

3. Results

3.1. Spectral analysis

Fig. 2 displays the brain topographic maps of the normalized mean EEG power in different frequency bands for ADHD and healthy control subjects. Specifically, the plots show that powers in $\boldsymbol{\theta}$ and $\boldsymbol{\beta}$ frequency bands in ADHD subjects are higher than that of the ones of the healthy subjects.

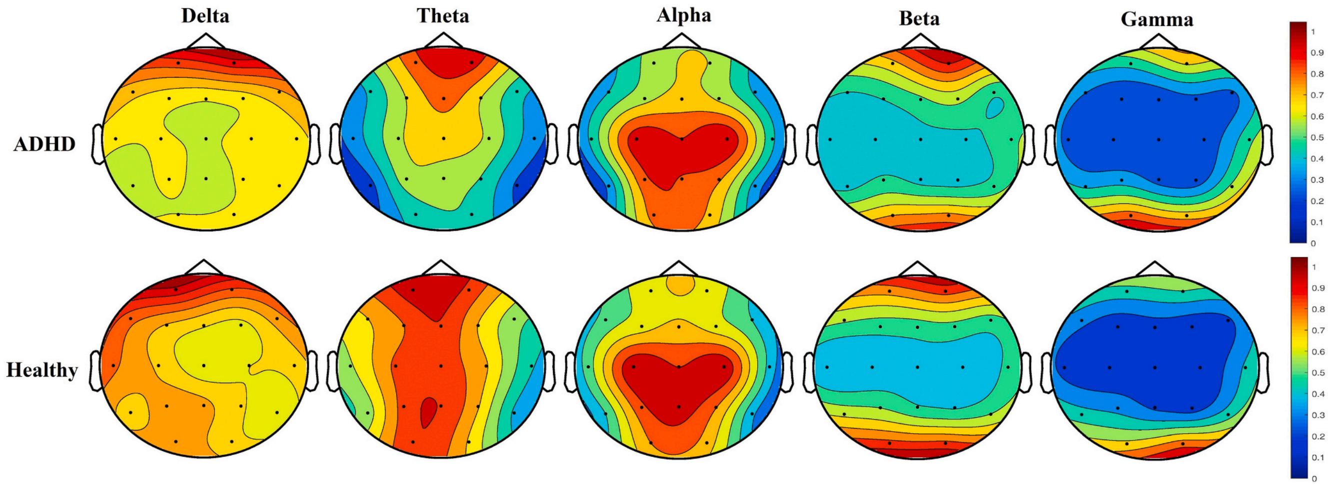

Fig. 2. Brain topographic maps of the normalized average EEG power in different frequency bands for ADHD and healthy control subjects.

3.2. Reaction time assessment

Fig. 3 shows the statistics of the response time recorded from the ADHD and healthy children. Note that the EEG database used in this study does not include the number of incorrect answers provided by the subjects. However, in [48], the number of incorrect answers for a subset of the database we have used in this study, i.e. 30 ADHD children and 30 healthy children, are reported to be 1.84 and 2.04 for healthy and ADHD subjects, respectively.

3.3. Effective BNs of ADHD and healthy control subjects

The first 1-min length of each 19-channel pre-processed EEG dataset was band-pass filtered in δ, θ, α, β and γ frequency bands and segmented in 3-s epochs with 1-s overlap. From each 3-s segment of multichannel EEG, five 19×19 graphs (i.e., CM's) representing directed BNs for each frequency band were computed using Eqs. (1)–(3). It resulted in 29 graphs for each EEG band for each dataset. In total, for each group, we computed $56 \times 29 = 1624$ graphs in each EEG rhythm. The averages of those 1624 graphs are shown in Fig. 4 and Fig. 5. The color-coded values in the graphs indicate the presence and strength of effective (directional) links between EEG electrodes and the flow of information among them.

3.4. Statistical analysis of connectivity measures for ADHD and healthy control subjects

The six directed graph measures described in Section 2.2.3 were extracted from each directed BN associated with the the EEG segments under analysis. As mentioned earlier, for each group, we had 1624 graphs in each frequency band. Therefore, for each graph measure in each of the five frequency bands, we had two 1×1624 vectors showing the values of that measure for the two groups. In order to statistically compare the values of the measures and check whether the values for the two groups are statistically different, we performed the independent two-sample t-test on the two vectors. The p-values are reported in Table 2 in which we have used * and ** to respectively indicate that p-value <0.05 and p-value <0.001.

Fig. 6 shows the box plots of all the six graph measures for the two groups in different EEG rhythms. Note that each box shows the distribution of a particular graph measure for a given group in a given frequency band through displaying the data quartiles and averages.

Finally, we evaluated the performance of each graph measure in classifying the BNs representing ADHD and healthy control subjects using the ROC analysis and the area under the ROC curve, i.e. the AUC, was used as a criterion of how well the measure differentiates between the two groups. The resulted AUC values are reported in Table 2.

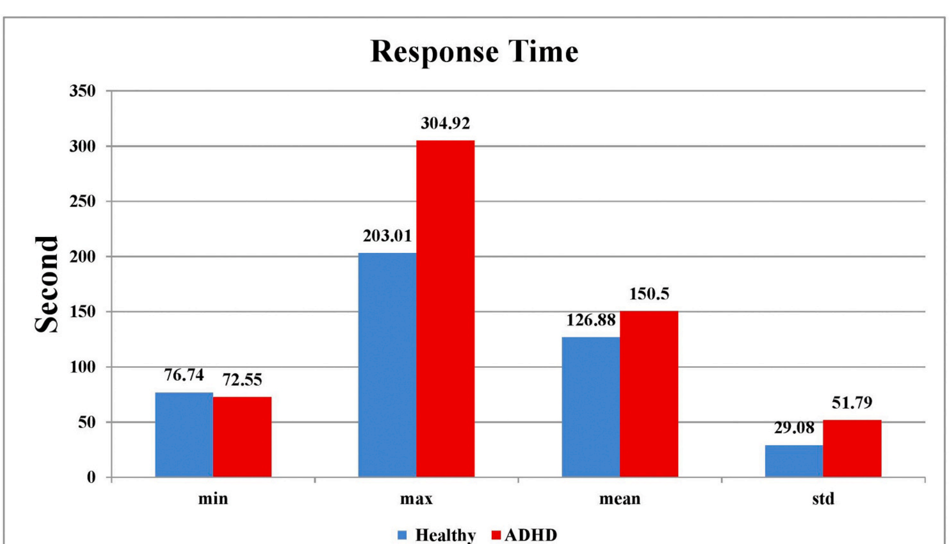

Fig. 3. Statistics of the response time for a subset of 30 ADHD and 30 healthy children in the EEG database, used in this study (see [48]).

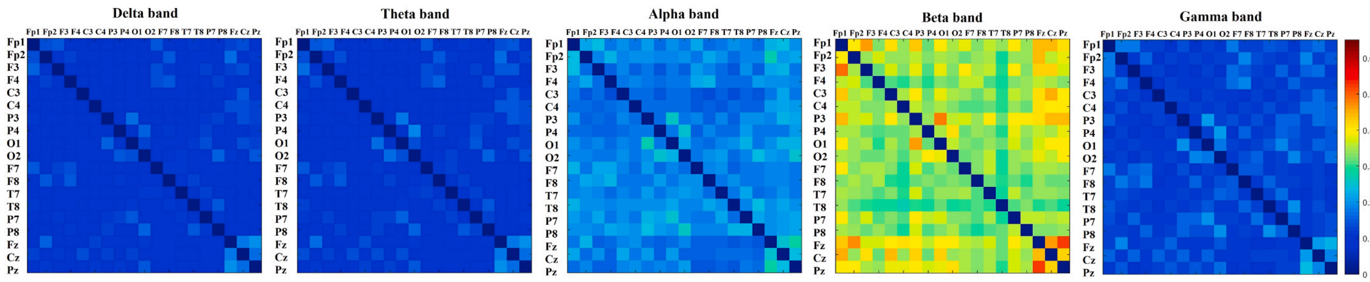

Fig. 4. The average of the connectivity matrices representing directed BNs in different frequency bands for ADHD subjects.

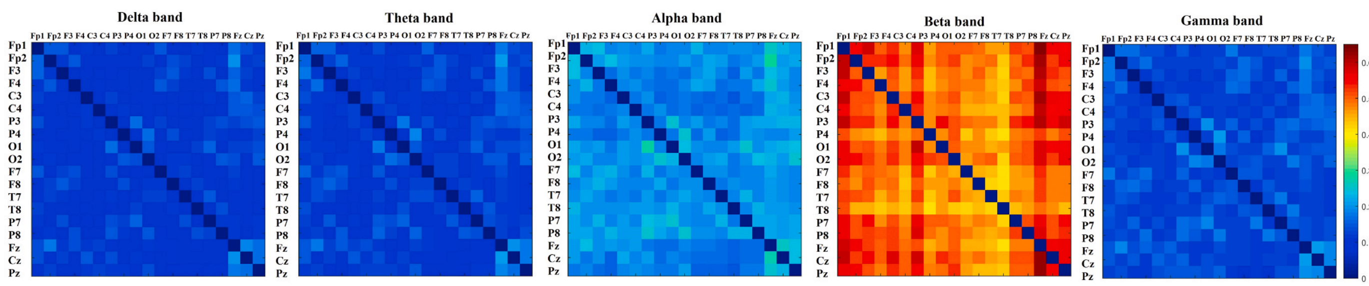

Fig. 5. The average of the connectivity matrices representing directed BNs in different frequency bands for healthy control subjects.

Table 2
Results of statistical and ROC analyses of the six graph measures used in this study to characterize the directed BNs in different frequency bands. The asterisks represent the significant values after *t*-test testing: * and ** respectively indicate that *p*-value <0.05 and *p*-value <0.001. Acronyms are as follows: GE: Global efficiency, MWCC: Mean weighted clustering coefficient, AD: Average degree, MS: Mean strength, Tr: Transitivity, and PL: Path length.

Frequency band	Delta		Theta		Alpha		Beta		Gamma	
	p-values	AUCs	*p*-values	AUCs	*p*-values	AUCs	*p*-values	AUCs	*p*-values	AUCs
GE	**	0.6090	**	0.6460	**	0.5253	**	0.7535	*	0.5188
MWCC	**	0.6013	**	0.6020	*	0.5270	**	0.7585	**	0.5395
AD	**	0.6194	**	0.6577	**	0.5294	**	0.7534	*	0.5181
MS	**	0.6194	**	0.6577	**	0.5294	**	0.7534	*	0.5181
Tr	**	0.6289	**	0.6670	**	0.5324	**	0.7525	*	0.5188
PL	**	0.6194	**	0.6577	**	0.5294	**	0.7534	*	0.5181

4. Discussion

The findings of this study are threefold: (i) transfer entropy can quantify the changes of effective brain connectivity as derived from scalp EEG signals at different frequency bands in children with ADHD; (ii) the most significant difference between the graph measures of effective brain connectivity of ADHD versus controls is reflected in the beta band of EEG; and (iii) this difference can be observed in different aspects of effective brain connectivity at the local and global scales. This finding is confirmed by the results of the ROC analysis given in Table 2 and visualized in Fig. 6. The AUC values and the box plots specifically show that graph measures extracted from the directed BNs in the β band are more discriminative between the two groups. According to Fig. 5, the most significant entropy values are across frontal areas and the spectral power is maximal at the beta band across the frontal and occipital areas. Interestingly, the average transfer entropy values of ADHD are significantly lower than the control group, which may imply that the information transfer across scalp EEG electrodes is impaired in ADHD.

The important role of EEG frequency bands and their relationship with different cognitive and behavioral abilities in humans has been widely studied [49,50]. In particular, the three frequency bands of δ, θ, and β have shown to be heavily related to concentration and relaxation. The δ band has been associated with deep sleep, interictal states, and sudden lapses of attention. The θ band is known to link with deep relaxation, dizziness, focus, balance and stability. The α band reflects wake and relaxed, calm states of mind, and high-level thinking such as mental calculations. The β band has been reported to be dominated in consciousness and awakeness, active concentration, motor activity as well as busy and anxious mental states. The results of this study put weight on the significance of the β band on the EEG recordings of ADHD in contrast to the other EEG frequency bands. As illustrated in Figs. 4 and 5, the highest discrimination between the graph features of effective connectivity in the ADHD and control groups are observed at the β frequency band. In other words, active concentration, motor activity, and anxiety are the most discriminative factors between the two groups. This is in line with our understanding from the impact of ADHD on children where they will face difficulties in the mental concentration abilities and may experience different levels of anxiety [51,52].

By using directed connectivity measures such as TE, one can take both directionality of information flow between different cortical areas and their network properties into account at the same time. The results of this study suggest that the direction of cortical interactions at the scalp level, measured by surface EEG, can provide useful information about ADHD and discriminate the associated brain dynamical states with the normal situation. In other words, the effective brain connectivity properties are affected by ADHD throughout EEG recordings. Having said that, one has to be aware of different interpretations between the effective connectivity analysis of EEG signals at the scalp level with the analysis of the reconstructed EEG signals at the source level or intracranial EEG recordings. The scalp EEG results must be interpreted

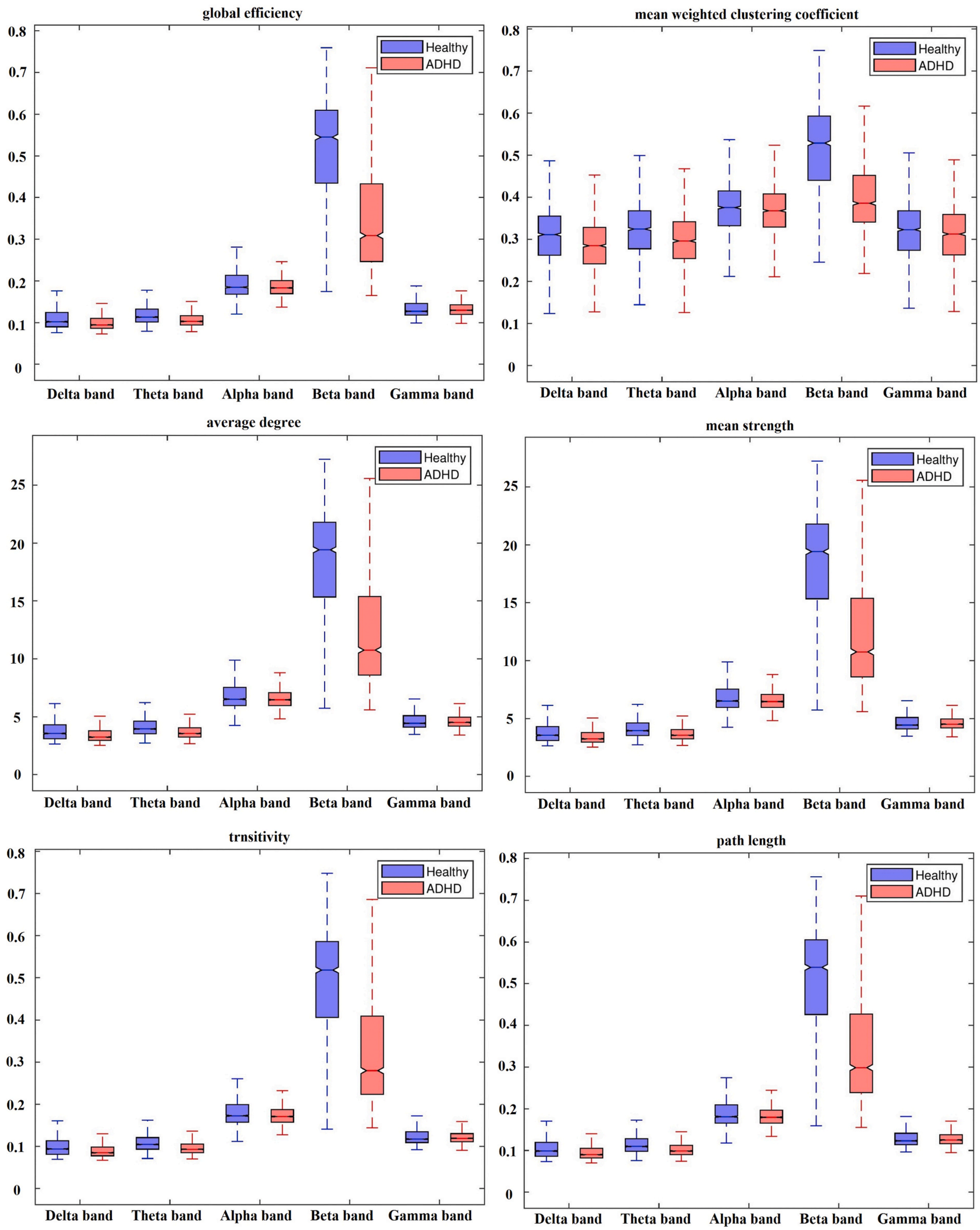

Fig. 6. Box plots showing the values of the six graph measures in different frequency bands for the ADHD and healthy control subjects.

with caution due the possible impact of volume conduction on the signals and possibly, spurious relationships across EEG channels. Therefore, the next step of this study would be to investigate the causal relationships between EEG signals in the ADHD cohort at the source level where we have a closer access to the electrical activity of neuronal populations within the cortex. Once this verification is made, the adapted methodology in this study will have the capacity to be used in the clinical settings. Potential applications may include the neurofeedback settings for ADHD patients and evaluation of the functional brain connections over time for monitoring any improvement over the course of treatment.

The cognitive visual task used in this study considers the behavior of ADHD children. The advantage of using a cognitive task in contrast to other types of stimuli such as sound is that an attention stimulus can highlight the potential difference between the ADHD group and control subjects better [36]. It is important to represent the ADHD children with some amusing images during the task engagement so that the pictures can stimulate a significant cognitive load in them. Our results suggest that the maximum discrimination between the two groups is reflected across the beta frequency band of EEG which is known to be associated with changes in brain states during demanding activities [53]. The continuous nature of visual stimuli in the design of the EEG datasets in this study can also help intensifying the impact of the cognitive load on the subjects throughout the entire EEG recording sessions. As Fig. 3 illustrates, the average response time in both groups has been comparable and also, the number of incorrect answers to the stimuli (1.84 in controls and 2.04 in ADHD subjects) has been close [35].

Previous studies have reported different contributions of EEG frequency bands in ADHD and there does not seem to be a consensus about the role of EEG band powers in ADHD so far. For example [54], has reported increased EEG power in alpha and beta bands of the ADHD group in contrast to controls. In [55], a greater alpha power was observed in the resting-state EEG datasets of children with ADHD. In [56], a significant increase in the beta band power was observed at the EEG source level and across temporal lobe in the ADHD group. The authors of [57] reported a significant increase in the EEG theta band of ADHD subjects, more than what was observed in the EEG beta band power (i.e., an increased theta to beta ratio in the ADHD group compared to controls). In addition, a machine learning study [58] suggested that the best predictor of ADHD status in EEG recordings is associated with an increased power in delta, theta and low-alpha over centro-parietal regions, and in frontal low-beta and parietal mid-beta. Our results, illustrated in Figs. 4, and Fig. 5, and Table 2, puts emphasis on the discriminative role of the theta and beta band in ADHD. Having said that, the beta band represents a much more pronounced impact on the graph features of functional BNs in our study (see Fig. 6). It may be due to the nature of event-related EEG recordings used in the analysis. According to [35], the EEG datasets have been recorded from ADHD/control participants while they have been exposed to a continuous cognitive visual task including multiple emotions. It may have activated different functional BNs and influenced EEG power across different frequency bands. Consequently, the graph features of EEG-based effective BNs may represent the impact of multiple cognitive and behavioral activities in the brain. The findings of this study are in line with the results of an independent study published in [33] while this manuscript was being revised.

5. Conclusion

This study supports the hypothesis that effective brain connectivity is altered in children with ADHD and the amount of information transfer between scalp EEG channels in those subjects is significantly different compared to healthy subjects. It demonstrates the potential of EEG-based effective brain connectivity analysis for diagnosis of ADHD. The results of this study put weight on the importance of beta band in scalp EEG recordings of ADHD and its impact on different network features of effective brain connectivity. The adapted methodology in this study is not limited to ADHD and could be used to investigate other brain abnormalities using EEG signals.

Declaration of competing interest

None declared.

Acknowledgements

A.O. acknowledges financial support through the Eurotech Postdoc Programme, co-funded by the European Commission under its framework programme Horizon 2020 (Grant Agreement number 754462).

References

[1] M.-D. Mălîia, et al., Functional mapping and effective connectivity of the human operculum, Cortex 109 (2018) 303–321.
[2] E. Allen, E. Damaraju, T. Eichele, L. Wu, V.D. Calhoun, EEG signatures of dynamic functional network connectivity states, Brain Topogr. 31 (1) (2018) 101–116.
[3] Z. Abbasvandi, A.M. Nasrabadi, A self-organized recurrent neural network for estimating the effective connectivity and its application to EEG data, Comput. Biol. Med. 110 (2019) 93–107.
[4] V.N. Vahia, Diagnostic and statistical manual of mental disorders 5: a quick glance, Indian J. Psychiatr. 55 (3) (2013) 220.
[5] J.A. King, M. Colla, M. Brass, I. Heuser, D.Y. von Cramon, Inefficient cognitive control in adult ADHD: evidence from trial-by-trial Stroop test and cued task switching performance, Behav. Brain Funct. 3 (1) (2007) 42.
[6] A. Corral, V. Espinoza, K. Yohannessen, P. Loyola, P. Balboa, C. Torrejón, Eating behavior disorders in patients hospitalized in a Mental Health Service, Rev. Chil. Pediatr. 90 (3) (2019) 302–308.
[7] M.R. Mohammadi, N. Malmir, A. Khaleghi, M. Aminiorani, Comparison of sensorimotor rhythm (SMR) and beta training on selective attention and symptoms in children with attention deficit/hyperactivity disorder (ADHD): a trend report, Iran. J. Psychiatry 10 (3) (2015) 165.
[8] C. Sridhar, S. Bhat, U.R. Acharya, H. Adeli, G.M. Bairy, Diagnosis of attention deficit hyperactivity disorder using imaging and signal processing techniques, Comput. Biol. Med. 88 (2017) 93–99.
[9] A.P. Association, Diagnostic and Statistical Manual of Mental Disorders-IV Text Revision, APA, Washington, DC, 2000.
[10] W.H. Organization, The ICD-10 Classification of Mental and Behavioural Disorders: Diagnostic Criteria for Research, World Health Organization, 1993.
[11] A. Omidvarnia, G. Azemi, B. Boashash, J.M. O'Toole, P.B. Colditz, S. Vanhatalo, Measuring time-varying information flow in scalp EEG signals: orthogonalized partial directed coherence, IEEE Trans. Biomed. Eng. 61 (3) (2013) 680–693.
[12] M. Pedersen, A. Zalesky, A. Omidvarnia, G.D. Jackson, Brain connectivity dynamics: multilayer network switching rate predicts brain performance, bioRxiv (2018) 403105.
[13] A. Sokolov Arseny, et al., Brain network analyses in clinical neuroscience, Swiss Archives of Neurology, Psychiatry and Psychotherapy 170 (6) (2019).
[14] K. Friston, C. Büchel, Attentional modulation of effective connectivity from V2 to V5/MT in humans, Proc. Natl. Acad. Sci. Unit. States Am. 97 (13) (2000) 7591–7596.
[15] R.A. Adams, M. Bauer, D. Pinotsis, K.J. Friston, Dynamic causal modelling of eye movements during pursuit: confirming precision-encoding in V1 using MEG, Neuroimage 132 (2016) 175–189.
[16] H.M. Chow, B. Kaup, M. Raabe, M.W. Greenlee, Evidence of fronto-temporal interactions for strategic inference processes during language comprehension, Neuroimage 40 (2) (2008) 940–954.
[17] A.A. Sokolov, P. Zeidman, M. Erb, P. Ryvlin, K.J. Friston, M.A. Pavlova, Structural and effective brain connectivity underlying biological motion detection, Proc. Natl. Acad. Sci. Unit. States Am. 115 (51) (2018) E12034–E12042.
[18] Y. Ren, et al., Effective connectivity of the anterior hippocampus predicts recollection confidence during natural memory retrieval, Nat. Commun. 9 (1) (2018) 1–10.
[19] N. Dijkstra, P. Zeidman, S. Ondobaka, M.A. van Gerven, K. Friston, Distinct top-down and bottom-up brain connectivity during visual perception and imagery, Sci. Rep. 7 (1) (2017) 1–9.
[20] M. Muthuraman, et al., Multimodal alterations of directed connectivity profiles in patients with attention-deficit/hyperactivity disorders, Sci. Rep. 9 (1) (2019) 1–13.
[21] C. Sripada, D. Kessler, Y. Fang, R.C. Welsh, K. Prem Kumar, M. Angstadt, Disrupted network architecture of the resting brain in attention-deficit/hyperactivity disorder, Hum. Brain Mapp. 35 (9) (2014) 4693–4705.
[22] G. Alba, et al., The variability of EEG functional connectivity of young ADHD subjects in different resting states, Clin. Neurophysiol. 127 (2) (2016) 1321–1330.
[23] A. Khadmaoui, et al., MEG analysis of neural interactions in attention-deficit/hyperactivity disorder, Comput. Intell. Neurosci. 2016 (2016).
[24] J. Wang, Functional Connectivity Analysis of Resting-State fMRI Data in ADHD Study, 2017.
[25] M. Ahmadlou, H. Adeli, Functional community analysis of brain: a new approach for EEG-based investigation of the brain pathology, Neuroimage 58 (2) (2011) 401–408.
[26] K. Krishnaveni, E. Radhamani, A study on brain network connectivity using neuroimaging techniques to diagnose ADHD, Composition theory XII (VIII August 2019).
[27] Z.-M. Wu, et al., Verbal working memory-related functional connectivity alterations in boys with attention-deficit/hyperactivity disorder and the effects of methylphenidate, J. Psychopharmacol. 31 (8) (2017) 1061–1069.
[28] R.B. Silberstein, A. Pipingas, M. Farrow, F. Levy, C.K. Stough, D.A. Camfield, Brain functional connectivity abnormalities in attention-deficit hyperactivity disorder, Brain and Behavior 6 (12) (2016), e00583.
[29] M. Murias, J.M. Swanson, R. Srinivasan, Functional connectivity of frontal cortex in healthy and ADHD children reflected in EEG coherence, Cerebr. Cortex 17 (8) (2007) 1788–1799.
[30] L. Michels, et al., Developmental changes of functional and directed resting-state connectivities associated with neuronal oscillations in EEG, Neuroimage 81 (2013) 231–242.
[31] H. Bakhshayesh, S.P. Fitzgibbon, A.S. Janani, T.S. Grummett, K.J. Pope, Detecting connectivity in EEG: a comparative study of data-driven effective connectivity measures, Comput. Biol. Med. 111 (2019) 103329.

[32] A.R. Anwar, et al., Effective connectivity of cortical sensorimotor networks during finger movement tasks: a simultaneous fNIRS, fMRI, EEG study, Brain Topogr. 29 (5) (2016) 645–660.
[33] A. Ekhlasi, A.M. Nasrabadi, M.R. Mohammadi, Direction of information flow between brain regions in ADHD and healthy children based on EEG by using directed phase transfer entropy, Cognitive Neurodynamics (2021) 1–12.
[34] M. Wibral, R. Vicente, M. Lindner, Transfer entropy in neuroscience, in: Directed Information Measures in Neuroscience, Springer, 2014, pp. 3–36.
[35] A.A. Ali Motie Nasrabadi, Mehdi Samavati, Mohammad Reza Mohammadi, EEG data for ADHD/Control children, IEEE Dataport, June 10 (2020).
[36] P. Jafari, A. Ghanizadeh, S. Akhondzadeh, M.R. Mohammadi, Health-related quality of life of Iranian children with attention deficit/hyperactivity disorder, Qual. Life Res. 20 (1) (2011) 31–36.
[37] F. Edition, Diagnostic and Statistical Manual of Mental Disorders, Am Psychiatric Assoc, 2013.
[38] V. Krishnaveni, S. Jayaraman, S. Aravind, V. Hariharasudhan, K. Ramadoss, Automatic identification and removal of ocular artifacts from EEG using wavelet transform, Meas. Sci. Rev. 6 (4) (2006) 45–57.
[39] T. Schreiber, Measuring information transfer, Phys. Rev. Lett. 85 (2) (2000) 461.
[40] C.J. Stam, E.A. De Bruin, Scale-free dynamics of global functional connectivity in the human brain, Hum. Brain Mapp. 22 (2) (2004) 97–109.
[41] X. Mao, P. Shang, Transfer entropy between multivariate time series, Commun. Nonlinear Sci. Numer. Simulat. 47 (2017) 338–347.
[42] J. Lee, S. Nemati, I. Silva, B.A. Edwards, J.P. Butler, A. Malhotra, Transfer entropy estimation and directional coupling change detection in biomedical time series, Biomed. Eng. Online 11 (1) (2012) 1–17.
[43] V. Latora, M. Marchiori, Efficient behavior of small-world networks, Phys. Rev. Lett. 87 (19) (2001) 198701.
[44] M. Girvan, M.E. Newman, Community structure in social and biological networks, Proc. Natl. Acad. Sci. U.S.A. 99 (2001) 8271–8276, cond-mat/0112110.
[45] D. Watts, S. Strogatz, Collective dynamics of "small-world" networks, Nature 393 (1998) 440–442, 46, View Article.
[46] Z. Dai, Y. He, Disrupted structural and functional brain connectomes in mild cognitive impairment and Alzheimer's disease, Neuroscience Bulletin 30 (2) (2014) 217–232.
[47] M. Rubinov, O. Sporns, Complex network measures of brain connectivity: uses and interpretations, Neuroimage 52 (3) (2010) 1059–1069.
[48] M.R. Mohammadi, A. Khaleghi, A.M. Nasrabadi, S. Rafieivand, M. Begol, H. Zarafshan, EEG classification of ADHD and normal children using non-linear features and neural network, Biomedical Engineering Letters 6 (2) (2016) 66–73.
[49] J.W. Britton, et al., Electroencephalography (EEG): an Introductory Text and Atlas of Normal and Abnormal Findings in Adults, Children, and Infants, American Epilepsy Society, Chicago, 2016.
[50] B.E.a.B.B. Itsu Sync, Different Types of Brain Waves: Delta, Theta, Alpha, Beta, Gamma, 18-Aug-2020. Available, https://itsusync.com/different-types-of-brain-waves-delta-theta-alpha-beta-gamma-ezp-9.
[51] E. Avni, E. Ben-Itzchak, D.A. Zachor, The presence of comorbid ADHD and anxiety symptoms in autism spectrum disorder: clinical presentation and predictors, Frontiers in Psychiatry, Original Research 9 (717) (2018-December-20 2018) (in English).
[52] A.J. McVey, et al., Social difficulties in youth with autism with and without anxiety and ADHD symptoms, Autism Res. 11 (12) (2018) 1679–1689.
[53] J. Baumeister, T. Barthel, K.-R. Geiss, M. Weiss, Influence of phosphatidylserine on cognitive performance and cortical activity after induced stress, Nutr. Neurosci. 11 (3) (2008) 103–110.
[54] S. Koehler, et al., Increased EEG power density in alpha and theta bands in adult ADHD patients, J. Neural. Transm. 116 (1) (2009) 97–104.
[55] M.M. Robertson, S. Furlong, B. Voytek, T. Donoghue, C.A. Boettiger, M. A. Sheridan, EEG power spectral slope differs by ADHD status and stimulant medication exposure in early childhood, J. Neurophysiol. 122 (6) (2019) 2427–2437.
[56] C.-T. Chiang, C.-S. Ouyang, R.-C. Yang, R.-C. Wu, L.-C. Lin, Increased temporal lobe beta activity in boys with attention-deficit hyperactivity disorder by LORETA analysis, Front. Behav. Neurosci. 14 (2020) 85.
[57] H. Heinrich, K. Busch, P. Studer, K. Erbe, G.H. Moll, O. Kratz, EEG spectral analysis of attention in ADHD: implications for neurofeedback training? Front. Hum. Neurosci. 8 (2014) 611.
[58] H. Kiiski, et al., EEG spectral power, but not theta/beta ratio, is a neuromarker for adult ADHD, Eur. J. Neurosci. 51 (10) (2020) 2095–2109.

Ali Kareem Abbas received his PhD in signal processing in 2020 from Razi University, Kermanshah, Iran. His main area of research is biomedical signal processing and neuroimaging.

Ghasem Azemi received his PhD degree in signal processing from Queensland University of Technology, Brisbane, Australia in 2004. He then joined the Faculty of Electrical and Computer Engineering Department of Electrical, Razi University, Kermanshah, Iran where he is now an Associate Professor. Between 2010 and 2014, he was with the Centre for Clinical Research, The University of Queensland, Brisbane, Australia as a Research Fellow. He is also holding an honorary Associate Professor position at the Department of Cognitive Science, Faculty of Medicine, Health and Human Sciences, Macquarie University, Sydney, Australia. His research interests include biomedical signal processing, neuroimaging and time–frequency signal processing.

Sajjad Amiri received his M.Sc degree in telecommunications engineering from Razi University, Kermanshah, Iran, in 2019. His areas of interests are signal processing, machine learning and graph analysis.

Samin Ravanshadi received his PhD degree from Sharif University of Technology in 2013. Since 2015, he has been with Razi University, Kermanshah, Iran, as an Assistant Professor. His research interests include modeling and control of physiological systems and biological signal processing.

Amir Omidvarnia received his BSc and MSc degrees both in Biomedical Engineering from Amirkabir University of Technology, Tehran, Iran, and the University of Tehran, Tehran, Iran (2002 and 2005, respectively). He then moved to the UK and Australia to pursue his studies. Awarded with a full International Postgraduate Research Scholarship, he obtained his PhD in Biomedical Signal Processing from The University of Queensland, Brisbane, Australia (2014). After his PhD he carried out a first postdoctoral research at the Florey Institute of Neuroscience and Mental Health, The University of Melbourne, Australia (2014–2019). He is currently doing his second postdoctoral research at the Medical Image Processing lab, Institute of Bioengineering, Ecole Polytechnique Fédérale de Lausanne, Geneva, Switzerland through a Marie-Curie EuroTech fellowship, awarded in 2019. His research interests include biomedical signal processing, neuroimaging and analysis of brain function.